Hindawi
Mathematical Problems in Engineering
Volume 2017, Article ID 7587294, 10 pages
https://doi.org/10.1155/2017/7587294

Research Article

Robust Master-Slave Synchronization of Neuronal Systems

Hector Puebla,[1] Eliseo Hernández-Martínez,[2] Mariana Rodriguez-Jara,[1] and Cesar S. Lopez-Monsalvo[3]

[1]*División de Ciencias Básicas e Ingeniería, Universidad Autónoma Metropolitana Azcapotzalco, Ciudad de México, Mexico*
[2]*Facultad de Ciencias Químicas, Universidad Veracruzana, Campus Xalapa, Xalapa, VER, Mexico*
[3]*Cátedras CONACyT, Universidad Autónoma Metropolitana Azcapotzalco, Ciudad de México, Mexico*

Correspondence should be addressed to Hector Puebla; hpuebla@correo.azc.uam.mx

Received 27 August 2017; Revised 4 December 2017; Accepted 11 December 2017; Published 28 December 2017

Academic Editor: Miguel A. F. Sanjuan

The desire to understand physiological mechanisms of neuronal systems has led to the introduction of engineering concepts to explain how the brain works. The synchronization of neurons is a central topic in understanding the behavior of living organisms in neurosciences and has been addressed using concepts from control engineering. We introduce a simple and reliable robust synchronization approach for neuronal systems. The proposed synchronization method is based on a master-slave configuration in conjunction with a coupling input enhanced with compensation of model uncertainties. Our approach has two nice features for the synchronization of neuronal systems: (i) a simple structure that uses the minimum information and (ii) good robustness properties against model uncertainties and noise. Two benchmark neuronal systems, Hodgkin-Huxley and Hindmarsh-Rose neurons, are used to illustrate our findings. The proposed synchronization approach is aimed at gaining insight into the effect of external electrical stimulation of nerve cells.

1. Introduction

Understanding how the brain works from a quantitative viewpoint is the domain of neural engineers [1]. Neural engineers apply mathematical and computational models, electrical engineering, and signal processing of living neuronal tissues [1, 2]. Two fundamental issues in neurosciences are the synchronization of individual neurons and the functional role of synchronized activity [3, 4]. Synchronization of neuron's activities is necessary for memory, calculation, motion control, and diseases such as epilepsy [5–8].

Synchronized activity and temporal correlation are critical for encoding and exchanging information for neuronal information processing in the brain [2–4]. Synchronization approaches in neuronal systems are aimed at exploring the communication between neurons with the computing of coupling functions that resemble observed experimental electrical cell activity [6–10]. From the general synchronization point of view, synchronization approaches can be classified into two general groups [11, 12]: (i) natural coupling (self-synchronization) [13–21] and (ii) artificial coupling using state observers or feedback control approaches [22–34].

Classical approaches to the problem of neuronal synchronization include diffusive and phase couplings [12–21]. Diffusive coupling via gap junctions is considered as the natural form of coupling in many neuronal processes [19–21]. Gap junctions can be written as a particular form of diffusive coupling. Phase coupling consists of modeling each member of the population as a phase oscillator and coupling them through the sine of their phase differences [21]. For instance, Wang et al. [19] applied phase differences to study different states of synchrony in two electrically coupled neurons.

From control engineering, two ways for synchronization of nonlinear systems, including the case of neuronal systems, are (i) observer-based synchronization [11, 12, 22], which uses state observers to synchronize nonlinear oscillators with the same order and structure, reaching identical synchronization, and (ii) controller-based synchronization [23–34], which uses control laws to achieve the synchronization between nonlinear oscillators, with different structure and order.

Control designs pose significant challenges due to the presence of disturbances, dynamic uncertainties, and nonlinearities in neuronal models. Indeed, neuronal models have significant structural and parametric uncertainties. For

instance, cell capacitances and resistances are obtained from biophysical data obtained from diverse sources [4, 35]. Moreover, experimental observations have pointed out that the synchronization phenomena in neuronal systems have robustness properties against cellular variability and intrinsic noise [36–40].

Relevant contributions addressing the synchronization of neuronal systems are the following. Aguilar-López and Martínez-Guerra [24] proposed a high order sliding mode controller that shows good robustness capabilities to external perturbations and internal noise. Bin et al. [25] introduced a backstepping control approach based on a Lyapunov function that achieves synchronization despite external disturbances. Based on feedback linearization ideas, Cornejo-Pérez and Femat [26] and Wang et al. [27, 28] introduced nonlinear controllers that achieve synchronization of coupled neurons despite external disturbances and unmeasured states. Nguyen and Hong [29] designed nonlinear and linear controllers with parameter adaptation to consider parameter uncertainties. They achieved synchronization of two coupled neurons. Using MPC and optimal controllers, Fröhlich and Jezernik [30, 31] designed controllers for the suppression of oscillations in neurons. Rehan et al. [23] and Rehan and Hong [32] proposed robust synchronization approaches using a linear matrix inequality controller and adaptation laws for uncertain parameters. Puebla et al. [33] introduced a robust feedback control scheme endowed with uncertainty compensation for regulation and tracking tasks in coupled neurons. Wang and Zhao [34] proposed a nonlinear model-based controller based on the inversion of the dynamics which guarantees the synchronization under no parametric uncertainties. Most of the above papers have addressed the robust synchronization problem of neuronal systems. However, their practical application is limited because of their structure and high computing cost as well as involved control designs.

A particular configuration for controller designs is the master-slave synchronization configuration, where the variable states of slave neurons are forced to follow the trajectories of a master neuron, which leads to an autonomous synchronization error. In this work, we address the master-slave synchronization of neuronal systems using a robust approach based on modeling error compensation (MEC) ideas [41]. There are different types of synchronization for coupled systems [11–13]. In this paper, synchronization of neuronal systems is defined as the match of the membrane potential. It is found that the MEC approach may achieve robust synchronization of the membrane potential via a coupling function also applied to the membrane potential. Numerical simulations on two benchmark neuronal systems show good performance of the robust synchronizer design.

The main contributions of this work can be summarized in four aspects. (i) We derive our control approach based on the direct dynamics of the master-slave synchronization error, leading to an autonomous tracking error and avoiding the change of coordinates as in feedback linearization and backstepping approaches. (ii) The proposed robust synchronization approach uses the minimum systems information (only the membrane potential measurement), and the coupling signal is also injected only to the membrane potential, facilitating its implementation in real systems. (iii) We use singular-perturbation theory as our main nonlinear stability tool [41, 42], including the effect of interconnection dynamics induced by model uncertainties. (iv) Our approach has a simple structure and provides good robustness against external perturbations and noise facilitating its physiological interpretation.

The rest of this work is organized as follows. In Section 2, we introduce two benchmark case studies of neuronal systems. In Section 3, the proposed robust master-slave synchronization is introduced. Section 4 presents the implementation and performance of the robust master-slave synchronization approach. Finally, in Section 5, we provide some concluding remarks.

2. Modeling Neurons

Mathematical modeling has made an enormous impact on neuroscience [1–4, 35]. A variety of dynamic models of the electrical activity of neurons have been reported in the literature [2–4, 43–46]. In this section, we introduce two benchmark case studies of neuronal systems: (i) the model proposed by Hodgkin and Huxley (HH) [35, 43–46], which is a realistic neuron model describing the propagation of an electric pulse along a squid axon membrane, and (ii) the Hindmarsh-Rose (HR) neuron model based on Hodgkin-Huxley type models describing the signal transmission across axons in neurobiology [2, 16, 35]. Based on the model structure of case studies, a general model of coupled or uncoupled neuronal systems is introduced. For completeness, we provide a brief introduction to the modeling of neurons.

2.1. Modeling the Electrical Activity of Neurons. The nervous system of an organism, which consists of neurons, is a communication network that allows for rapid transmission of information between cells [2, 16, 35]. A neuron receives information through the dendrites which are transported via axons, which provide links to other neurons via synapses [2, 16]. The transport of ions of sodium and potassium through the outer membrane of a nerve cell is responsible for electrical signals that transmit information to other neurons [2, 16].

Neurons are excitable media and respond to electrical stimuli, and this response is exploited when studying neurons. After a low impact of electric current, the excitable cells relax immediately to their initial state. If a pulse exceeds a threshold value, a single nerve pulse appears on the excitable membrane of the nerve tissue (action potential) that propagates along the nerve, preserving constant amplitude and form [2, 16, 35].

The propagation mechanism of an electric pulse along a membrane axon is associated with the fact that the permittivity of a membrane depends on existing currents and voltages and is different for different ions [43–45]. In particular, sodium and potassium ions are fundamental in the functioning of a neuron [2, 16, 35]. The cell membrane of a neuron is impermeable to sodium and potassium ions when the cell is in a resting state. An inactive neuron has a resting potential, which is generated via a transport protein called the sodium-potassium pump. This protein moves sodium ions outside the

cell and simultaneously moves some potassium ions into the cell's cytoplasm. Thus, the cell is more positive outside than inside, due to the fact that the number of sodium ions moved outside the cell is greater than the number of potassium ions moved inside. When a stimulus arrives at the nerve cell, its surface becomes permeable to sodium ions, which flows into the cells, resulting in a reversal of polarization. The interior of the cell becomes positively charged, and the outside becomes negatively charged. Then, the interior becomes permeable to potassium which flows outside through potassium channels, reversing the polarization of the cell below the polarization of the resting state. To restore that polarization, the excess of the cell sodium (at the interior) and potassium (at the exterior) is pumped [2, 16, 35, 43–46].

HH described the action potential wave of excited squid giant axons with an external electrical signal via a set of mathematical equations [2, 16, 35, 43–46]. At present, it is still the basic model for describing such phenomena [2, 16, 35]. The HH model for excitability in the membrane of the squid giant axon is complicated and consists of one nonlinear partial differential equation coupled to three ordinary differential equations [43–45].

In the early 1960s, FitzHugh applied model reduction techniques to the analysis of the HH equations [45]. That reduction of the HH equations later became known as the FitzHugh-Nagumo (FHN) model and had given a great insight into the mathematical and physiological complexities of the excitability process [2, 16, 45]. The FHN model reduction uses the fact that the time scales of the two channels are quite different. Sodium channel had a faster time scale than potassium channel. Thus, the sodium channel can always be considered in equilibrium, reducing the HH model to two equations [45]. Thus, FHN model is an approximation to the HH model retaining essential features of the action potential.

2.2. HH Neuron Model. The HH neurons are usually used as realistic models of neuronal systems, for studying neuronal synchronization. The HH model describes how action potentials in neurons are initiated and propagated and approximates the electrical characteristics of excitable cells [44]. The HH model for two neurons is described by the following set of eight ordinary differential equations (ODEs) [2, 16, 35]:

$$\begin{aligned}
\frac{dx_{M,1}}{dt} &= -\frac{1}{C_{m,M}}\left(g_{\mathrm{k},M}x_{M,2}^2\left(x_{M,1}-x_{M,1\mathrm{k}}\right)\right.\\
&\quad + g_{\mathrm{Na},M}x_{M,3}x_{M,4}\left(x_{M,1}-x_{M,1\mathrm{Na}}\right)\\
&\quad \left. + g_{\mathrm{l},M}\left(x_{M,1}-x_{M,1\mathrm{l}}\right)\right) + \frac{1}{C_{m,M}}I_M,\\
\frac{dx_{M,2}}{dt} &= \alpha_{n,M}\left(x_{M,1}\right)\left(1-x_{M,2}\right)-\beta_{n,M}\left(x_{M,1}\right)x_{M,2},\\
\frac{dx_{M,3}}{dt} &= \alpha_{m,M}\left(x_{M,1}\right)\left(1-x_{M,3}\right)-\beta_{m,M}\left(x_{M,1}\right)x_{M,3},\\
\frac{dx_{M,4}}{dt} &= \alpha_{h,M}\left(x_{M,1}\right)\left(1-x_{M,4}\right)-\beta_{h,M}\left(x_{M,1}\right)x_{M,4},\\
\frac{dx_{S,1}}{dt} &= -\frac{1}{C_{m,S}}\left(g_{\mathrm{k},S}x_{S,2}^2\left(x_{S,1}-x_{S,1\mathrm{k}}\right)\right.\\
&\quad + g_{\mathrm{Na},S}x_{S,3}x_{S,4}\left(x_{S,1}-x_{S,1\mathrm{Na}}\right)+g_{\mathrm{l},S}\left(x_{S,1}-x_{S,1\mathrm{l}}\right)\Big)\\
&\quad + \frac{1}{C_{m,S}}I_S,\\
\frac{dx_{S,2}}{dt} &= \alpha_{n,S}\left(x_{S,1}\right)\left(1-x_{S,2}\right)-\beta_{n,S}\left(x_{S,1}\right)x_{S,2},\\
\frac{dx_{S,3}}{dt} &= \alpha_{m,S}\left(x_{S,1}\right)\left(1-x_{S,3}\right)-\beta_{m,S}\left(x_{S,1}\right)x_{S,3},\\
\frac{dx_{S,4}}{dt} &= \alpha_{h,S}\left(x_{S,1}\right)\left(1-x_{S,4}\right)-\beta_{h,S}\left(x_{S,1}\right)x_{S,4},
\end{aligned} \tag{1}$$

where $x_{i,1}$, $x_{i,2}$, $x_{i,3}$, and $x_{i,4}$ (subindices $i = M, S$ denote master and slave neurons) represent the membrane potential, the activation of the potassium flow current, and the activation and inactivation of the sodium flow current, respectively. $C_{m,i}$ is the membrane capacitance, $g_{\mathrm{k},i}$, $g_{\mathrm{Na},i}$, and $g_{\mathrm{l},i}$ are the maximum ionic and leak conductance, and $x_{i,1\mathrm{k}}$, $x_{i,1\mathrm{Na}}$, and $x_{i,1\mathrm{l}}$ stand for the ionic and leak reversal potentials [2, 4, 16, 39]. I_i is the external stimulus current. The functions $\alpha_{j,i}(x_{i,1})$ and $\beta_{j,i}(x_{i,1})$ describe the transition rates between open and closed states of the channels.

2.3. Hindmarsh-Rose Neurons. As a second case study, we consider a benchmark Hindmarsh-Rose (HR) neuron model, which can be seen as a physiologically realistic model of the HH type describing the signal transmission across axons in neurobiology [2, 16, 35]. Under external current stimulation, the individual HR model may show chaotic behavior. The model of two uncoupled HR neurons is described as

$$\begin{aligned}
\frac{dx_{M,1}}{dt} &= x_{M,2}-a_Mx_{M,1}^3+b_Mx_{M,1}^2-x_{M,3}+I_M,\\
\frac{dx_{M,2}}{dt} &= c_M-d_Mx_{M,1}^2-x_{M,1},\\
\frac{dx_{M,3}}{dt} &= r_M\left[s_M\left(x_{M,1}-x_{M,10}\right)-x_{M,3}\right],\\
\frac{dx_{S,1}}{dt} &= x_{S,2}-a_Sx_{S,1}^3+b_Sx_{S,1}^2-x_{S,3}+I_S,\\
\frac{dx_{S,2}}{dt} &= c_S-d_Sx_{S,1}^2-x_{S,1},\\
\frac{dx_{S,3}}{dt} &= r_S\left[s_S\left(x_{S,1}-x_{S,10}\right)-x_{S,3}\right],
\end{aligned} \tag{2}$$

where $x_{i,1}$ is the membrane potential, $x_{i,2}$ is associated with the fast current Na^+ or K^+, and $x_{i,3}$ is associated with the slow current, for example, Ca^{2+}. I is the external current input.

2.4. A General Model of Synchronized Neuronal Systems. We consider a general class of master-slave configuration of

neuronal systems coupled through the membrane potential, that is, $x_{i,1}$. The dynamics of the master neuron are modeled as

$$\begin{aligned} \frac{dx_{M,1}(t)}{dt} &= f_{M,1}\left(x_M(t)\right), \\ \frac{dx_{M,j}(t)}{dt} &= f_{M,j}\left(x_M(t)\right), \end{aligned} \tag{3}$$

where $x_{M,1}(t)$ denotes the membrane potential of the master neuron and $x_{M,j}(t)$ are the remaining states of the master neuron.

The dynamics of the slave neuron are modeled as

$$\begin{aligned} \frac{dx_{S,1}(t)}{dt} &= f_{S,1}\left(x_S(t)\right), \\ \frac{dx_{S,j}(t)}{dt} &= f_{S,j}\left(x_S(t)\right), \end{aligned} \tag{4}$$

where $x_{S,1}(t)$ denotes the membrane potential of the slave neuron and $x_{S,j}(t)$ are the remaining states of the slave neuron.

Coupled neurons can be modeled as

$$\begin{aligned} \frac{de(t)}{dt} &= \frac{dx_{S,1}(t)}{dt} - \frac{dx_{M,1}(t)}{dt} \\ &= f_{S,1}\left(x_S(t)\right) - f_{M,1}\left(x_M(t)\right) + u(t), \end{aligned} \tag{5}$$

where $e(t)$ denotes the synchronization error and $u(t)$ is an external electrical input applied to the slave neuron.

The following comments are in order:

(i) The original HH model is given by coupled nonlinear ODEs which are a simplification of full partial differential equations (PDEs) that describes the neuron membrane [2, 16, 35, 43–46]. Both HH and HR neuron models can reproduce its main features when they are exposed to an external current (existence of an excitation threshold, relative and absolute refractory periods, and the generation of pulse trains). Thus, for synchronization design purposes, benchmark models with small dimension and less complexity are more suitable.

(ii) The external input $u(t)$ represents an externally applied current into the cell from an electrode. The membrane voltage can also be readily measured, and the controller can be realized easily using this combination of input-output variables. The use of an external current as the manipulable variable is realistic since it has a significant effect on the dynamics of membrane potential leading to depolarization and repolarization of the neuron [2, 4]. On the other hand, several experimental studies have shown that the synchronization of coupled neurons depends on external stimulus properties [10, 13–15].

(iii) Uncertainties in neuron models arise in two main ways: structural and parametric [35, 40, 43]. Structural uncertainty refers to different choices of fitting of sodium and potassium conductance curves in a model. The uncertainty that arises from the approximation of complex models to simpler ones also fits into the category of model uncertainty. Parametric uncertainty refers to variation in the numerical base values of different parameters of the model. These parameters may include changes due to intrinsic electric and magnetic properties of tissue. For instance, each neuron may have a different set of conductances [16, 35, 40]. Moreover, the thermal motion of the molecules leads to noise and fluctuations in the variables of the model [36–39].

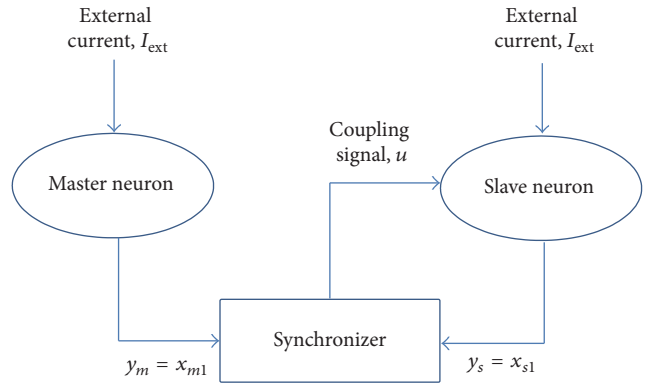

Figure 1: Master-slave synchronization of neuronal systems.

3. Robust Master-Slave Synchronization

In this section, based on modeling error compensation (MEC) ideas, the synchronizer design is presented. First, the problem is stated as a master-slave configuration, and some assumptions for the synchronizer design are introduced. Next, robustness and stability issues of the synchronization approach are provided.

3.1. Synchronization Problem. The synchronization problem is stated as follows; that is, the output of a master neuron is the reference of a slave neuron so that the output of the slave system follows the output of the master system asymptotically. We apply an external signal at the slave neuron to track the desired behavior of the master neuron. Figure 1 shows the scheme of the synchronization approach.

The following assumptions complete the synchronization problem description:

(A1) Nonlinear functions $f_{M,1}(x_M)$ and $f_{S,1}(x_S)$ are smooth functions.

(A2) The general coupled neuron model given by (5) is affected by uncertainties and external perturbations with bounded variation.

(A3) The measurement of the membrane voltage in the master and slave neurons is available for synchronization design purposes.

The following comments are in order:

(i) (A1) is realistic. Indeed, the primary source of nonlinearity in neuron models is the conductance curves, which meet these assumptions [2, 16, 35].

(ii) (A2) considers that the coupled neuron model contains uncertainties related to uncertain parameters and unmodeled dynamics, that is, $\pi(t) + \xi(y(t))$. As stated in the above section, functions $f_{M,1}(x_M)$ and $f_{S,1}(x_S)$ can contain uncertain parameters, or, in the worst case, the whole terms are unknown. Indeed, the parameters in neuron models have some degree of uncertainty, as these parameter values are commonly estimated from experimental data, which contain errors due to both the estimation procedure adopted to fit data and the experimental errors of the data themselves [35, 40, 43].

3.2. Robust Synchronization Design. The synchronizer design consists of the following steps.

(1) Consider the coupled neurons model given by (5):

$$\begin{aligned}\frac{de(t)}{dt} &= \frac{dx_{S,1}(t)}{dt} - \frac{dx_{M,1}(t)}{dt} \\ &= f_{S,1}\left(x_S(t)\right) - f_{M,1}\left(x_M(t)\right) + u(t).\end{aligned} \tag{6}$$

(2) Lump the uncertain terms in a single new state $\eta(t)$ [33, 34]. From the model given by (5) and assumptions (A1) and (A2), the modeling error $\eta(t)$ and the equivalent model are written as

$$\begin{aligned}\eta(t) &= f_{S,1}\left(x_S(t)\right) - f_{M,1}\left(x_M(t)\right), \\ \frac{de(t)}{dt} &= \eta(t) + u(t).\end{aligned} \tag{7}$$

(3) Estimate the uncertain term $\eta(t)$ via a reduced order observer [33, 34]:

$$\frac{d\eta(t)}{dt} = \tau_e^{-1}\left(\eta(t) - \overline{\eta(t)}\right); \tag{8}$$

introducing $\omega(t) = \tau_e\overline{\eta}(t) - y(t)$, the reduced order observer can be written as follows:

$$\frac{d\omega(t)}{dt} = u(t) - \overline{\eta(t)}, \tag{9}$$

where τ_e is the only observer design parameter. In the context of control theory, the reduced observer can be seen as a signal estimator, where the modeling error signal is seen as an additional state. In this way, the estimation of the modeling error endows the control system with robustness against model uncertainties.

(4) Design a synchronizer to drive the synchronization error to zero with the dynamics given by

$$\frac{de(t)}{dt} = \tau_c^{-1}e(t) \tag{10}$$

which is obtained using the following coupling input:

$$u(t) = -\tau_c^{-1}e(t) + \eta(t), \tag{11}$$

where τ_c is the synchronizer design parameter. In this way, the asymptotic convergence $e(t) \to 0$, and so $x_{S,1}(t) \to x_{M,1}(t)$, is guaranteed.

The resulting synchronizer depends only on the measures of the membrane voltages in the master and slave neurons and the estimated value of the lumped uncertain terms $\overline{\eta}(t)$. It is also noted that the proposed synchronizer has only two parameters, one for the observer and the other for the coupling input $u(t)$.

The tuning of both parameters follows a simple rule [41]: $\tau_p > 0.5\tau_c > 0.5\tau_e$, where τ_p is the inverse of the dominant oscillation frequency of the master neuron, τ_c can be seen as a synchronization time constant which is tuned to get a satisfactory synchronization performance, and τ_e determines the smoothness of the modeling error estimation.

3.3. Robustness and Stability Properties. To obtain satisfactory and practical synchronization strategies, they should be robust in response to both model uncertainties and external perturbations. The robustness properties against model uncertainties of the proposed synchronizer design are related to the compensation of the estimated lumped uncertain terms.

The stability analysis of the proposed synchronizer design is based on singular-perturbation arguments [41, 42]. For the sake of completeness in presentation, a sketch of main ideas of the stability results for the MEC approach is provided as follows [34].

Given the synchronization error $e(t)$ and defining the estimation error as $\phi(t) = \eta(t) - \overline{\eta(t)}$, then the synchronized system becomes

$$\begin{aligned}\frac{de(t)}{dt} &= -\tau_c^{-1}e(t) + \phi(t), \\ \frac{d\phi(t)}{dt} &= -\tau_e^{-1}\phi(t) + \Gamma\left(e(t), \phi(t)\right),\end{aligned} \tag{12}$$

where $\Gamma(e(t), \phi(t))$ stands for the time derivative of lumped uncertain terms, which does not depend on τ_e. By assumptions (A1) and (A2), it can be shown that such time derivative is a continuous function of its arguments. Thus, there exist two positive constants ν_1 and ν_2 both independent of τ_e, such that

$$\left|\Gamma\left(e(t), \phi(t)\right)\right| \le \nu_1 |e(t)| + \nu_2 \left|\phi(t)\right|. \tag{13}$$

The synchronized system can be seen as a nonlinear singularly perturbed system with τ_e as the perturbation parameter and $e(t)$ and $\phi(t)$ as the slow and fast variables, respectively [42]. The reduced system (obtained by taking $\tau_e = 0$) and the boundary-layer system (obtained by taking the time-scaling $t' = t/\tau_e$ and $\tau_e = 0$) are linearly asymptotically stable. Hence, there exists a maximum estimation time constant τ_e^*, such that for all $\tau_e < \tau_e^*$ the regulation error $e(t)$

goes asymptotically to zero. The maximum estimation time constant can be taken as a measure of the robustness of the proposed synchronizer. Larger values of $\tau_e{}^*$ lead to better robustness capabilities. Smaller values of τ_e lead to a faster estimation of the modeling error. However, excessively small values of τ_e must be avoided in practice, since measurement noise and unmodeled high-frequency dynamics (e.g., actuator dynamics and dead-time) impose limitations on the estimator bandwidth. Stability results imply that perturbations, noise, and fluctuations with bounded variations do not affect the stability of synchronizer design.

4. Numerical Studies

In this section, simulation results are presented for the synchronization of the case studies. First, the proposed synchronizer approach is presented for three sets of synchronizer parameters $[\tau_c, \tau_e]$. Next, robustness capabilities against model parameters uncertainties are considered. Finally, the synchronization capabilities are evaluated concerning random fluctuations on the slave's membrane potential.

4.1. Synchronization of HH Neurons. We consider two HH neurons with the following form of the functions $\alpha_i(x_1)$ and $\beta_i(x_1)$ $(i = n, m, h)$, which describes the transition rates between open and closed states of the channels [4]:

$$\begin{aligned}
\alpha_n(x_1) &= \frac{0.01\,(10 - x_1)}{\exp\left[(10 - x_1)/10\right] - 1},\\
\beta_n(x_1) &= 0.125\exp\left(\frac{-x_1}{80}\right),\\
\alpha_m(x_1) &= \frac{0.1\,(25 - x_1)}{\exp\left[(25 - x_1)/10\right] - 1},\\
\beta_m(x_1) &= 4\exp\left(\frac{-x_1}{18}\right),\\
\alpha_h(x_1) &= 0.07\exp\left(\frac{-x_1}{20}\right),\\
\beta_h(x_1) &= \frac{1}{\exp\left[(20 - x_1)/10\right] + 1}.
\end{aligned} \tag{14}$$

Other model parameters for the base numerical simulation are [19, 25] $x_{M,1\mathrm{Na}} = x_{S,1\mathrm{Na}} = 115.0$ mV, $x_{M,1\mathrm{l}} = x_{S,1\mathrm{l}} = 10.599$ mV, $x_{M,1\mathrm{k}} = 7.2$ mV, $x_{M,1\mathrm{k}} = -12.0$ mV (representing the equilibrium potentials of the sodium, leak, and potassium, resp.), $g_{\mathrm{Na},M} = g_{\mathrm{Na},S} = 120.0\,\mathrm{ms/cm}^2$, $g_{\mathrm{L},M} = g_{\mathrm{L},S} = 0.3\,\mathrm{ms/cm}^2$, and $g_{\mathrm{K},M} = 12.0\,\mathrm{ms/cm}^2$, $g_{\mathrm{K},M} = 36.0\,\mathrm{ms/cm}^2$ (representing the maximum conductance of the corresponding ionic currents), $C_M = C_S = 1.0\,\mathrm{F/cm}^2$ (membrane capacitance), $I_M = 3.18$, and $I_S = 80$ (externally applied currents). Numerical simulations were performed using a fourth-order Runge-Kutta integration algorithm which was programmed in Matlab software v.7, with an integration step of 0.1 and the following initial conditions: $(x_{M,1}(0), x_{M,2}(0), x_{M,3}(0), x_{M,4}(0)) = (0.1, 0.1, 0.01, 0.1)$ and $(x_{S,1}(0), x_{S,2}(0), x_{S,3}(0), x_{S,4}(0)) = (50, 0.5, 0.2, 0.5)$.

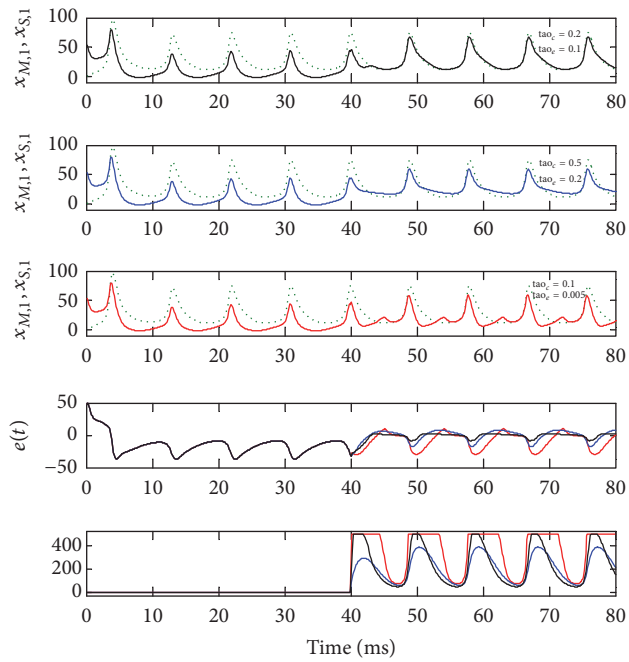

FIGURE 2: Synchronization of HH neurons for three sets of synchronizer parameters.

4.1.1. Synchronization of Two HH Neurons. Figure 2 shows the synchronization results for three different sets of the synchronizer parameters $[\tau_c, \tau_e]$: (a) base parameters $[0.2, 0.1]$ (continuous black line), (b) higher control parameters $[0.5, 0.2]$ (continuous blue line), and (c) smaller control parameters $[0.1, 0.05]$ (continuous red line). The coupling input is switched on at time $t = 40$ ms. To consider realistic values of applied external current, minimum and maximum values of the coupling input u are set as $u_{\min} = 0$ and $u_{\max} = 500$.

As shown in Figure 2, HH neurons exhibit different simple periodic dynamical behavior before the activation of the synchronizer. After the proposed synchronizer approach is applied, synchronization errors converge to zero. It is observed that the synchronization error is lower for the base synchronizer parameters. The slight mismatch between the slave and master state is due to the saturation of the coupling function. Lower values of the synchronizer parameters induce a significant mismatch due to the high intensity of the coupling function that stays most of the time at the upper saturation level. On the other hand, larger values of synchronizer parameters show a minor effort of the coupling input, but in this case also a significant mismatch is observed.

From Figure 2, it can be observed that high values of the external coupling function are required to synchronize the membrane potential. This is in accordance with theoretical and experimental observations, where it has been reported that in HH neurons a small external applied current results in a small net current that drives the membrane potential to rest (repolarization) [4, 43]. Thus, intermediate to high external applied currents produce perturbations required to achieve the synchronization.

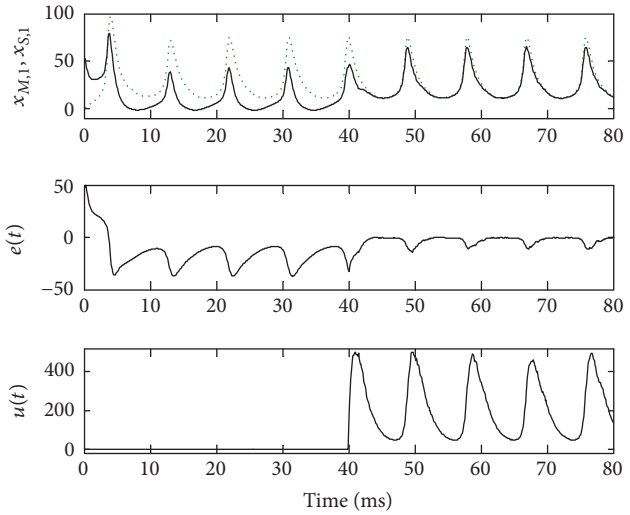

FIGURE 3: Robustness of the synchronization of HH neurons against parameter mismatch.

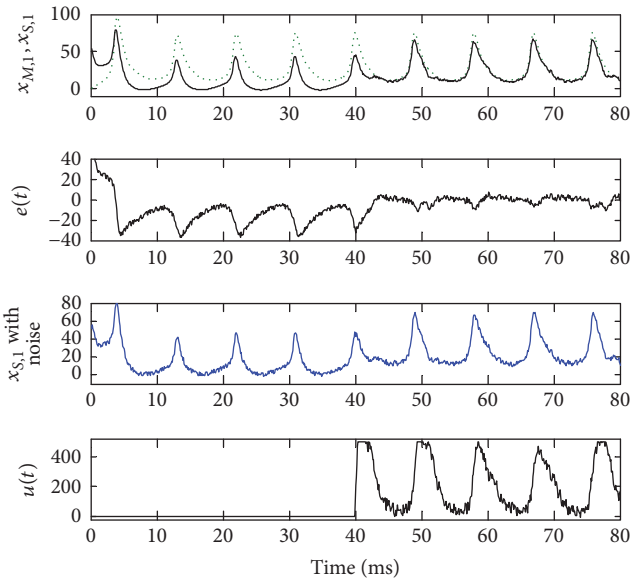

FIGURE 4: Robustness of the synchronization of HH neurons against noise.

4.1.2. Robustness against Uncertain Model Parameters and Membrane Potential Fluctuations. The robustness capabilities of the MEC synchronization scheme against parameter mismatch and fluctuations in the membrane potential are evaluated as follows. (i) A random parameter mismatch of 5% between master and slave neurons is first considered. (ii) A random fluctuation of 10% was added in the membrane potential of the slave neuron. The above perturbations are simulated with Gaussian random noise, which is usually used to simulate most common disturbances in neuroscience [4, 35]. Synchronizer parameters are set as the base values of Figure 2.

The simulation results are shown in Figures 3 and 4. A similar synchronization error is noted as in the case of identical parameters, only with slight distortions of the coupling function. Thus, it can be observed that the performance of the synchronization scheme shows good robustness capabilities to random perturbations.

4.2. Synchronization of HR Neurons. For the second case study, we consider two HR neurons. Base parameter values are [13, 21] $a_m = a_s = 1$, $b_m = b_s = 3$, $c_m = c_s = 1$, $d_m = d_s = 5$, $s_m = s_s = 4$, $r_m = r_s = 0.006$, $I_m = 3.2$, and $I_s = 2.8$. The minimum value of the coupling input in this case is $u_{\min} = -2.8$, such that the minimum external current to the slave neuron is zero. In this case, numerical simulations were also performed using a fourth-order Runge-Kutta integration algorithm programmed in Matlab v.7, with an integration step of 0.1 and the following initial conditions: $(x_{M,1}(0), x_{M,2}(0), x_{M,3}(0)) = (0.1, 0.1, 0.1)$ and $(x_{S,1}(0), x_{S,2}(0), x_{S,3}(0)) = (0.2, 0.2, 0.2)$.

4.2.1. Synchronization of Two HR Neurons. Figure 5 shows numerical results for two neurons and three different sets of the synchronizer parameters $[\tau_c, \tau_e]$: (a) base parameters [1, 0.5] (continuous black line), (b) higher control parameters

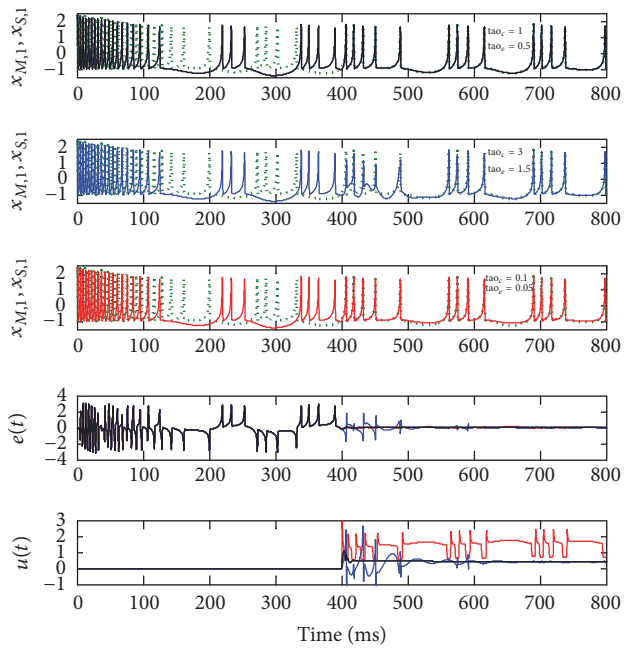

FIGURE 5: Synchronization of HR neurons for three sets of synchronizer parameters.

[3, 1.5] (continuous blue line), and (c) smaller control parameters [0.1, 0.05] (continuous red line). The coupling input is switched on at time $t = 400$ ms. It can be observed from Figure 5 that before the synchronizer is implemented master and slave neurons exhibit chaotic dynamical behaviors and are not synchronized.

Figure 5 shows that, for nominal and small synchronizer parameters, the synchronization error dynamics go quickly to zero. On the other hand, for higher synchronizer parameter values, the synchronization error also vanishes but after a

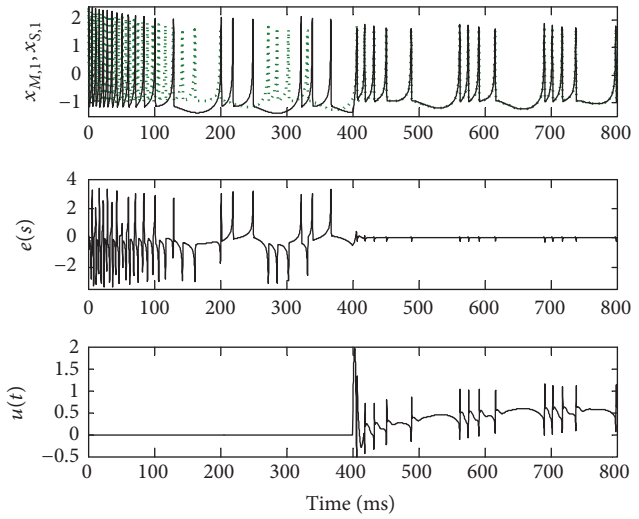

Figure 6: Robustness of the synchronization of HR neurons against parameter mismatch.

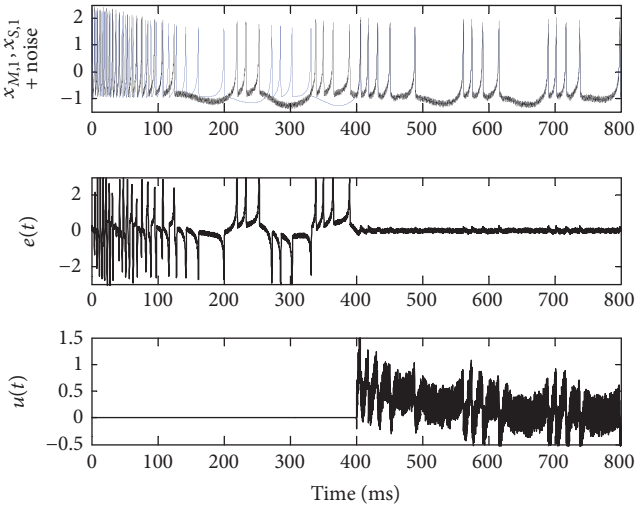

Figure 7: Robustness of the synchronization of HR neurons against noise.

significant transitory dynamic. Notice that the required coupling functions for lower and higher synchronizer parameters show oscillatory behaviors. In particular, the effect of small synchronizer parameters leads to an increase of oscillatory behavior due to the high sensitivity of the proposed estimator.

4.2.2. Robustness against Uncertain Model Parameters and Membrane Potential Fluctuations. Figures 6 and 7 show, for the base parameter values of the synchronizer, the robustness capabilities of the synchronization approach to parameter mismatch and measurement potential fluctuations. In both cases, almost complete synchronization is achieved. Figure 6 shows that to suppress parameter uncertainties the coupling input requires significant effort in the regions of spiking behavior of the neurons. On the other hand, the effect of measurement noise is also reflected in the coupling input,

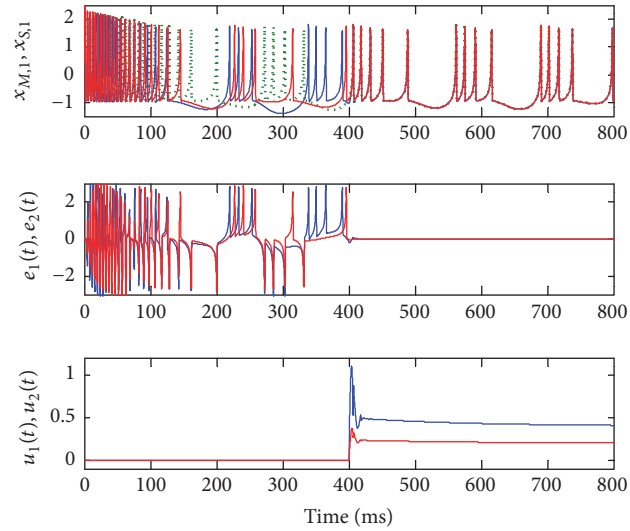

Figure 8: Synchronization of three HR neurons.

which shows a noisy behavior and a lower strength than the case of noiseless measurements, reflecting some behavior observed in real neurons [36–39].

4.2.3. Synchronization of Three HR Neurons. The extension of the proposed synchronizer approach for three coupled neurons (i.e., two slave neurons) is illustrated in Figure 8. In this case, initial conditions for the second slave neuron are $(x_{S2,1}(0), x_{S2,2}(0), x_{S2,3}(0)) = (0.15, 0.15, 0.15)$, and $I_{s2} = 3$. We have used nominal synchronizer parameters.

Figure 8 shows the synchronization error for both slave neurons. It is noted that the synchronizer approach can drive the synchronization errors to zero. The corresponding coupling inputs show a slight oscillation with a fast convergence to a flat ramp. Then, we can establish that the proposed synchronization approach can be applied to multiple neurons.

5. Conclusions

This paper introduces a robust approach for synchronization of neuronal systems. Using a master-slave configuration, we provide robustness capabilities via the lumping, estimation, and compensation of model uncertainties. The coupling function computing via the synchronization approach uses only the membrane potential and is only also applied to the membrane potential of the neuron, resembling the strength of electrical gap junctions. Synchronization dynamics are analyzed using stability arguments of nonsingular perturbation systems. The performance of the proposed synchronization approach is validated through in-depth numerical simulations on two benchmark models of neuronal systems. Furthermore, since our approach uses the minimum model information, the proposed method can be applied for synchronization of more complex and multiple neuronal systems. Our study aims to contribute to the understanding of both processes that influence the synchronization of

individual neurons and the functional role of synchronized activity of coupled neurons in neural and mental disorders.

Conflicts of Interest

The authors declare that they have no conflicts of interest.

References

[1] C. Eliasmith and C. H. Anderson, *Neural Engineering: Computation, Representation, and Dynamics in Neurobiological Systems*, Computational Neuroscience Series, MIT Press, Cambridge, Mass, USA, 2004.

[2] J. Keener and J. Sneyd, *Mathematical Physiology: I: Cellular Physiology*, Interdisciplinary Applied Mathematics, Springer Science & Business Media, New York, NY, USA, 2010.

[3] B. Gutkin, D. Pinto, and B. Ermentrout, "Mathematical neuroscience: from neurons to circuits to systems," *Journal of Physiology-Paris*, vol. 97, no. 2-3, pp. 209–219, 2003.

[4] E. M. Izhikevich, *Dynamical Systems in Neuroscience: the Geometry of Excitability And Bursting*, MIT Press, Cambridge, Mass, USA, 2007.

[5] P. Fries, "A mechanism for cognitive dynamics: neuronal communication through neuronal coherence," *Trends in Cognitive Sciences*, vol. 9, no. 10, pp. 474–480, 2005.

[6] C. M. Gray, "Synchronous oscillations in neuronal systems: mechanisms and functions," *Journal of Computational Neuroscience*, vol. 1, no. 1-2, pp. 11–38, 1994.

[7] C. Hammond, H. Bergman, and P. Brown, "Pathological synchronization in Parkinson's disease: networks, models and treatments," *Trends in Neurosciences*, vol. 30, no. 7, pp. 357–364, 2007.

[8] E. Niebur, S. S. Hsiao, and K. O. Johnson, "Synchrony: a neuronal mechanism for attentional selection?" *Current Opinion in Neurobiology*, vol. 12, no. 2, pp. 190–194, 2002.

[9] R. Ritz and T. J. Sejnowski, "Synchronous oscillatory activity in sensory systems: new vistas on mechanisms," *Current Opinion in Neurobiology*, vol. 7, no. 4, pp. 536–546, 1997.

[10] P. A. Tass, "Effective desynchronization with a stimulation technique based on soft phase resetting," *EPL (Europhysics Letters)*, vol. 57, no. 2, pp. 164–170, 2002.

[11] L. M. Pecora and T. L. Carroll, "Synchronization of chaotic systems," *Chaos: An Interdisciplinary Journal of Nonlinear Science*, vol. 25, no. 9, Article ID 097611, 2015.

[12] S. Boccaletti, J. Kurths, G. Osipov, D. L. Valladares, and C. S. Zhou, "The synchronization of chaotic systems," *Physics Reports*, vol. 366, no. 1-2, pp. 1–101, 2002.

[13] L. Glass, "Synchronization and rhythmic processes in physiology," *Nature*, vol. 410, no. 6825, pp. 277–284, 2001.

[14] D. di Bernardo and M. G. Signorini, "A model of two nonlinear coupled oscillators for the study of heartbeat dynamics," *International Journal of Bifurcation and Chaos*, vol. 08, no. 10, pp. 1975–1985, 1998.

[15] R. C. Elson, A. I. Selverston, R. Huerta, N. F. Rulkov, M. I. Rabinovich, and H. D. I. Abarbanel, "Synchronous behavior of two coupled biological neurons," *Physical Review Letters*, vol. 81, no. 25, pp. 5692–5695, 1998.

[16] C. P. Fall, E. S. Marland, J. M. Wagner, and J. J. Tyson, *Computational Cell Biology*, vol. 20 of *Interdisciplinary Applied Mathematics*, Springer-Verlag, New York, NY, USA, 2002.

[17] R. E. Mirollo and S. H. Strogatz, "Synchronization of pulse-coupled biological oscillators," *SIAM Journal on Applied Mathematics*, vol. 50, no. 6, pp. 1645–1662, 1990.

[18] J.-W. Shuai and D. M. Durand, "Phase synchronization in two coupled chaotic neurons," *Physics Letters A*, vol. 264, no. 4, pp. 289–297, 1999.

[19] J. Wang, W. Ye, S. Liu, B. Lu, and X. Jiang, "Qualitative and quantitative aspects of synchronization in coupled CA1 pyramidal neurons," *Chaos, Solitons & Fractals*, vol. 93, pp. 32–38, 2016.

[20] Q. Y. Wang, Q. S. Lu, G. R. Chen, and D. H. Guo, "Chaos synchronization of coupled neurons with gap junctions," *Physics Letters A*, vol. 356, no. 1, pp. 17–25, 2006.

[21] Y. Kuramoto, *Chemical Oscillations, Waves and Turbulence*, Springer, New York, NY, USA, 1984.

[22] H. Nijmeijer and I. M. Mareels, "An observer looks at synchronization," *IEEE Transactions on Circuits and Systems I: Fundamental Theory and Applications*, vol. 44, no. 10, pp. 882–890, 1997.

[23] M. Rehan, K. Hong, and M. Aqil, "Synchronization of multiple chaotic FitzHugh-Nagumo neurons with gap junctions under external electrical stimulation," *Neurocomputing*, vol. 74, no. 17, pp. 3296–3304, 2011.

[24] R. Aguilar-López and R. Martínez-Guerra, "Synchronization of a coupled Hodgkin-Huxley neurons via high order sliding-mode feedback," *Chaos, Solitons & Fractals*, vol. 37, no. 2, pp. 539–546, 2008.

[25] D. Bin, W. Jiang, and F. Xiangyang, "Synchronizing two coupled chaotic neurons in external electrical stimulation using back-stepping control," *Chaos, Solitons & Fractals*, vol. 29, no. 1, pp. 182–189, 2006.

[26] O. Cornejo-Pérez and R. Femat, "Unidirectional synchronization of Hodgkin-Huxley neurons," *Chaos, Solitons & Fractals*, vol. 25, no. 1, pp. 43–53, 2005.

[27] J. Wang, T. Zhang, and Y. Che, "Chaos control and synchronization of two neurons exposed to ELF external electric field," *Chaos, Solitons & Fractals*, vol. 34, no. 3, pp. 839–850, 2007.

[28] J. Wang, T. Zhang, and B. Deng, "Synchronization of FitzHugh-Nagumo neurons in external electrical stimulation via nonlinear control," *Chaos, Solitons & Fractals*, vol. 31, no. 1, pp. 30–38, 2007.

[29] L. H. Nguyen and K.-S. Hong, "Adaptive synchronization of two coupled chaotic Hindmarsh-Rose neurons by controlling the membrane potential of a slave neuron," *Applied Mathematical Modelling*, vol. 37, no. 4, pp. 2460–2468, 2013.

[30] F. Fröhlich and S. Jezernik, "Feedback control of Hodgkin-Huxley nerve cell dynamics," *Control Engineering Practice*, vol. 13, no. 9, pp. 1195–1206, 2005.

[31] F. Fröhlich and S. Jezernik, "Annihilation of single cell neural oscillations by feedforward and feedback control," *Journal of Computational Neuroscience*, vol. 17, no. 2, pp. 165–178, 2004.

[32] M. Rehan and K. Hong, "LMI-based robust adaptive synchronization of FitzHugh-Nagumo neurons with unknown parameters under uncertain external electrical stimulation," *Physics Letters A*, vol. 375, no. 15, pp. 1666–1670, 2011.

[33] H. Puebla, R. Aguilar-Lopez, E. Ramirez-Castelan, E. Hernandez-Martinez, and J. Alvarez-Ramirez, "Control and synchronization of Hodgkin-Huxley neurons," in *BIOMAT 2009*, pp. 125–135, World Scientific Publishing Co., Hackensack, NJ, USA, 2010.

[34] X. Wang and Q. Zhao, "Tracking control and synchronization of two coupled neurons," *Nonlinear Analysis: Real World Applications*, vol. 11, no. 2, pp. 849–855, 2010.

[35] E. de Schutter, *Computational Modeling Methods for Neuroscientists*, Computational Neuroscience, The MIT Press, Cambridge, Mass, USA, 2009.

[36] P. Parmananda, C. H. Mena, and G. Baier, "Resonant forcing of a silent Hodgkin-Huxley neuron," *Physical Review E: Statistical, Nonlinear, and Soft Matter Physics*, vol. 66, Article ID 047202, 2002.

[37] W. Wang, Y. Wang, and Z. D. Wang, "Firing and signal transduction associated with an intrinsic oscillation in neuronal systems," *Physical Review E: Statistical, Nonlinear, and Soft Matter Physics*, vol. 57, no. 3, pp. R2527–R2530, 1998.

[38] Y. G. Yu, W. Wang, J. F. Wang, and F. Liu, "Resonance-enhanced signal detection and transduction in the Hodgkin-Huxley neuronal systems," *Physical Review E: Statistical, Nonlinear, and Soft Matter Physics*, vol. 63, no. 2, pp. 1–12, 2001.

[39] A. Mikhailov and B. Hess, "Fluctuations in living cells and intracellular traffic," *Journal of Theoretical Biology*, vol. 176, no. 1, pp. 185–192, 1995.

[40] M. S. Goldman, J. Golowasch, E. Marder, and L. F. Abbott, "Global structure, robustness, and modulation of neuronal models," *Journal of Neuroscience*, vol. 21, no. 14, pp. 5229–5238, 2001.

[41] J. Alvarez-Ramírez, "Adaptive control of feedback linearizable systems: a modelling error compensation approach," *International Journal of Robust and Nonlinear Control*, vol. 9, no. 6, pp. 361–377, 1999.

[42] F. Hoppensteadt, "Asymptotic stability in singular perturbation problems. II: problems having matched asymptotic expansion solutions," *Journal of Differential Equations*, vol. 15, pp. 510–521, 1974.

[43] M. Girardi-Schappo, M. H. R. Tragtenberg, and O. Kinouchi, "A brief history of excitable map-based neurons and neural networks," *Journal of Neuroscience Methods*, vol. 220, no. 2, pp. 116–130, 2013.

[44] A. L. Hodgkin and A. F. Huxley, "A quantitative description of membrane current and its application to conduction and excitation in nerve," *The Journal of Physiology*, vol. 117, no. 4, pp. 500–544, 1952.

[45] R. Fitzhugh, "Impulses and physiological states in theoretical models," *Biophysical Journal*, vol. 1, pp. 445–466, 1961.

[46] T. D. Sangrey, W. O. Friesen, and W. B. Levy, "Analysis of the optimal channel density of the squid giant axon using a reparameterized Hodgkin-Huxley model," *Journal of Neurophysiology*, vol. 91, no. 6, pp. 2541–2550, 2004.